Geomechanics and Engineering, *Vol. 14, No. 3 (2018) 271-281*
DOI: https://doi.org/10.12989/gae.2018.14.3.271

Numerical investigations on stability evaluation of a jointed rock slope during excavation using an optimized DDARF method

Yong Li[*1,2], Hao Zhou[1,3a], Zhenxing Dong[1b], Weishen Zhu[1c], Shucai Li[1d] and Shugang Wang[1e]

[1]*Geotechnical & Structural Engineering Research Center, Shandong University, No. 17923 Jingshi Rd., Jinan, Shandong Province, P. R. China 250061*
[2]*School of Civil Engineering, Shandong University, No. 17922 Jingshi Rd., Jinan, Shandong Province, P. R. China 250061*
[3]*Jinan Rail Transit Group Co., Ltd, No. 2000 Shunhua Rd., Jinan, Shandong Province, P. R. China 250101*

(Received December 8, 2016, Revised June 26, 2017, Accepted July 24, 2017)

Abstract. A jointed rock slope stability evaluation was simulated by a discontinuous deformation analysis numerical method to investigate the process and safety factors for different crack distributions and different overloading situations. An optimized method using Discontinuous Deformation Analysis for Rock Failure (DDARF) is presented to perform numerical investigations on the jointed rock slope stability evaluation of the Dagangshan hydropower station. During the pre-processing of establishing the numerical model, an integrated software system including AutoCAD, Screen Capture, and Excel is adopted to facilitate the implementation of the numerical model with random joint network. These optimizations during the pre-processing stage of DDARF can remarkably improve the simulation efficiency, making it possible for complex model calculation. In the numerical investigations on the jointed rock slope stability evaluations using the optimized DDARF, three calculation schemes have been taken into account in the numerical model: (I) no joint; (II) two sets of regular parallel joints; and (III) multiple sets of random joints. This model is capable of replicating the entire processes including crack initiation, propagation, formation of shear zones, and local failures, and thus is able to provide constructive suggestions to supporting schemes for the slope. Meanwhile, the overloading numerical simulations under the same three schemes have also been performed. Overloading safety factors of the three schemes are 5.68, 2.42 and 1.39, respectively, which are obtained by analyzing the displacement evolutions of key monitoring points during overloading.

Keywords: jointed rock mass; slope stability; numerical investigation; DDARF; overloading test

1. Introduction

In China, hydraulic engineering has achieved great and rapid progress since the 1950s. It is anticipated that, in the twenty-first century, the hydropower exploitation would gain an even greater breakthrough by two stages (Peng 2006, Zhu 2009). The first decade of the twenty-first century is the first stage. During this stage, the national hydropower capacity had reached 210, 000 MW by the end of 2010, and the hydropower energy occupied about 30% of the national electric supply. The second stage is from 2011 to 2050, under the national great strategies such as 'Western development' (Shih 2004) and 'One belt and one road' (Liu 2015), China will make full use of the hydropower energy. Tens of large-scale hydropower stations will be built in the south western areas. For example, the Motuo hydropower station in Tibet, with design installed generator capacity larger than 40,000 MW, will be put into operation in the second stage. Rock slope can be often found in vicinity of hydraulic structures, and it is a typical of geological entity located on the surface of earth crust, which is composed of sloping surfaces, slope top, slope shoulder, slope foot, and slope entity of definite depth (Yan *et al.* 2000, Zaruba and Mencl 1969). The integral stability of rock slope will give rise to significant influences on construction, normal running and safety of the project (Ministry of Water Resources of the People's Republic of China 2007, Li *et al.* 2015). The narrow and steep terrains between Tibetan Plateau and Sichuan Basin are prone to large-scale slope instabilities (Huang 2009). Previous slope instable accidents have occurred in this area with complex geological conditions (Dai *et al.* 2005, Yin *et al.* 2009, Huang and Fan 2013, Xu *et al.* 2013, Qi *et al.* 2015, Terzi and Selcuk 2015). Therefore, rock slope stability evaluation has become a vital problem in geotechnical engineering practices (Yang *et al.* 2015, Sarfarazi *et al.* 2016).

The approaches of rock stability analysis can be divided into two types. The first type is named qualitative analytical methodology, which consists of geologic history mechanism analysis and engineering geologic analogism.

∗Corresponding author, Associate Professor
E-mail: yongli@sdu.edu.cn
[a]M.Sc.
E-mail: haozhouchina@gmail.com
[b]M.Sc. Candidate
E-mail: 296294042@qq.com
[c]Professor
E-mail: zhuw@sdu.edu.cn
[d]Professor
E-mail: lishucai@sdu.edu.cn
[e]Professor
E-mail: shugangwang@gmail.com

ISSN: 2005-307X (Print), 2092-6219 (Online)

The second type is named quantitative analytical methodology, which consists of limit equilibrium analysis and numerical analysis (Duncan 1996). As for the qualitative analytical methodology, it is most important to help practical engineers in originally estimating the rock slope stability, especially during the phases of renaissance and planning while the comprehensive factors could be considered. However, experimental investigations as well as numerical simulations are not necessarily demanded in these phases. Therefore, quantitative analytical methodology is most popular and comprehensively applied in the rock slope stability evaluations.

As for the quantitative analytical methodology, previous methods can be divided into four categories (Yang and Yin 2004, Li *et al.* 2009): (1) the limit equilibrium method; (2) the characteristic line method; (3) the limit analysis method; and (4) numerical techniques. The limit equilibrium methods including the conventional slices methods have been widely applied due to their simplicity and applicability mainly applied to soil slopes (Bishop and Morgenstern 1960, Morgenstern and Price 1965, Spencer 1967, Janbu 1973, Sarma 1973, Florkiewicz and Kubzdela 2013, Guharay and Baidya 2014, Yang and Pan 2015, Zhao *et al.* 2015, Cemalettin *et al.* 2016, Gao *et al.* 2016). The safety factor obtained by the first three methods are always not uniquely determined as it often changes with the assumption proposed for the slip surface, and the calculation results could not be reasonable if the discontinuities cannot be neglected in the slope rock mass. Owing to the fact that numerical methods can consider complex geological conditions of rock slope, such as complex geometry, anisotropy characteristics and nonlinear behaviors of rock mass, they have become increasingly important. If the failure mechanism of slope is not controlled by the discontinuities, the continuous numerical methods can be used to perform the rock slope stability analysis, which includes finite element method (FEM) (Ji and Liao 2014, Jiang *et al.* 2015, Liu *et al.* 2015), finite different method (FDM) (Latha and Garaga 2010, Xiao *et al.* 2015) and block element method (BEM) (Chen *et al.* 2003, Wang and Ni 2013). Actually, the rock slope in southwestern China always contains numerous discontinuities, which may result in large block movement. Under these complex geological conditions, the discontinuous numerical methods are most appropriate in the stability evaluations of jointed rock slope. For example, the discrete element method (DEM) (Cundall and Strack 1979, Lu *et al.* 2014, Bonilla-Sierra *et al.* 2015), particle flow code (PFC) (Wang *et al.* 2003, Zhao *et al.* 2015), universal distinct element method (UDEC) (Choi and Chung 2004, Hungr *et al.* 2011, Nichol *et al.* 2011, Günther *et al.* 2012) and discontinuous deformation analysis (DDA) (Hatzor *et al.* 2003, Sun *et al.* 2011, Chen *et al.* 2013, Jiao *et al.* 2014a) have all been employed to carry out the stability analysis of jointed rock slope. Jiao *et al.* (2014b) proposed a Discontinuous Deformation Analysis for Rock Failure (DDARF) to simulate the shear behavior and even the hydraulic fracturing of jointed rock mass. Li *et al.* (2016) used DDARF to numerically simulate the shear behaviors of jointed rock mass. The unique advantage of DDARF is that it can numerically simulate the whole failure process of jointed rock mass, including the crack initiation, propagation and coalescence and the eventual failure. More researchers simulated laboratory experiments rather than existing engineering on account of some shortcomings of this program. Therefore, the DDARF method needs improving to simulate existing engineering projects, such as slope and underground openings. In this paper, an optimized DDARF is proposed to enlarge the application extent of DDARF, while it can satisfy the requirements for calculation accuracy and efficiency. Then, it is used to perform numerical investigations on the jointed rock slope stability evaluation of the Dagangshan hydropower station, which is located in Sichuan province, China.

2. Introduction of principles for an optimized DDARF

Discontinuous Deformation Analysis (DDA) method, initially proposed by Shi (1988) is widely used to perform the stability analysis of jointed rock mass. It follows the fundamental theories of elasticity and the FEM, and can also solve the large deformation problems in jointed rock mass as the DEM does. However, as the rock blocks are entirely discrete, sometimes it cannot numerically simulate the whole failure process of jointed rock mass. Therefore, a developed numerical method named DDARF is proposed (Zhang 2007, Jiao *et al.* 2010, Jiao *et al.* 2014b) to analyze the failure problems of jointed rock mass. However, this DDARF can only establish a numerical model that uses uniformly distributed grids, and the numerical calculation cannot be completed if the number of elements is larger than several thousands. Therefore, in this paper, an optimized DDARF associated with Auto CAD is proposed to overcome the disadvantages in DDARF.

2.1 Generation of random joint network

It is believed that the joints distribution in natural rock mass often obeys macroscopic statistical laws. And the corresponding geometrical parameters of rock joints (including trace length, dip angle and dip strike) are often presumed to conform to a mathematical model, such as lognormal distribution, normal distribution, uniform distribution, and negative exponential distribution, etc. Former researchers have verified that the Monte-Carlo method (e.g., Zheng *et al.* 2015) can successfully describe the corresponding geometrical parameters.

The detailed steps on generating a random joint network are demonstrated as follows (Zhang *et al.* 2008):

(1) As for each joint set, repeat the following steps;

(2) Evaluate the number of the random joints (N) in the simulated area by the following formula

$$N = \frac{S}{d \cdot l} \tag{1}$$

where S denotes the area of the numerical model, d denotes the average value of joint spacings, and l representsthe average value of joint trace lengths;

(3) A sequence of N random numbers of uniform distribution will be expressed by an equation using linear congruent method;

(4) Following the same way as step (3), the direction angles of N joints and joint trace length with normal distribution will be determined;

(5) Based on the joint geometrical parameters, the coordinates of two end points of each joint can be calculated;

(6) For each joint, the two end points need to be checked whether they are beyond the area of interest. If yes, the outside section will be cut off, and correspondingly the coordinates of the end point will be changed.

2.2 Generation of random joint network

The joint network consists of a number of randomly distributed joints, most of which are non-persistent. According to the joint network, a travelling wave method (Yu *et al.* 2010) is employed to generate the triangular block system automatically.

Initially, the Monte-Carlo method is employed to generate the random joint network in the simulated area. Then, according to the joint network, artificial joints for each single endpoint till the whole simulated area are divided into a number of single-connected subdomains. Finally, all of the subdomains are searched and meanwhile the travelling wave method is employed to generate the triangular blocks in each subdomain. Consequently, the triangular block system has been completed in DDARF.

2.3 Cracking algorithm of artificial joints

When generating the triangular block system, numerous artificial joints are simultaneously shaped, and they can supply the potential routes along which the cracks initiate, spread, and even propagate. The physico-mechanical properties for artificial joints are determined by the strength parameters of intact rock in order to represent the characteristics of the continuous areas. Rock failure is induced by ruptures of some artificial joints, which is controlled by the maximum tensile stress condition expressed in Eq. (2) and Mohr-Coulomb criterion expressed in Eq. (3)

$$f_n = -\sigma_t \cdot l \tag{2}$$

$$f_\tau = C \cdot l + f_n \cdot \tan\varphi \tag{3}$$

where f_n and f_τ denote the normal contact force and tangential contact force, respectively; σ_t denotes the uniaxial tensile strength; C denotes the cohesion; φ denotes the internal friction angle; and l denotes the length of contact.

In case one of Eqs. (2) and (3) is satisfied, the artificial joints will be developed to be actual joints.

2.4 The optimized DDARF

As mentioned above, not only does DDARF make full use of the advantages of DDA, but also can numerically simulate the whole failure process of jointed rock mass. It can be used for both intact and jointed rock mass. However, it also has one disadvantage in the pre-processing stage. In DDARF, the geometry information of the numerical model should be input manually, which will cost a lot of unnecessary workload. To optimize the tedious pre-processing stage, a useful software named AutoCAD, which

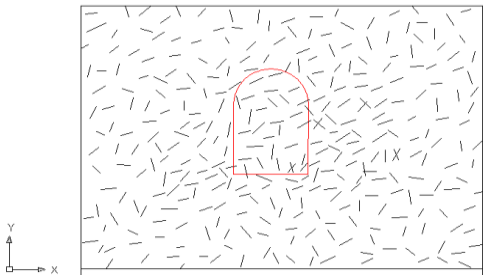

Fig. 1 Schematic of the numerical model for an underground cavern with random joint group

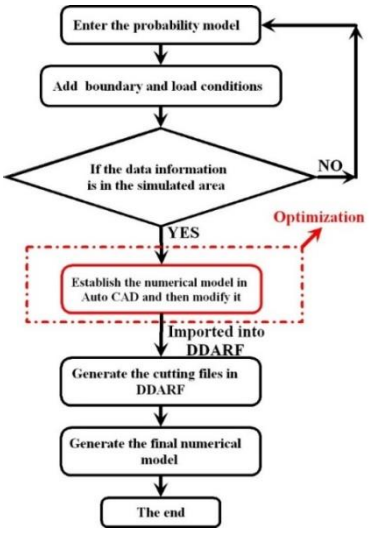

Fig. 2 A technical flowchart for the optimized DDARF

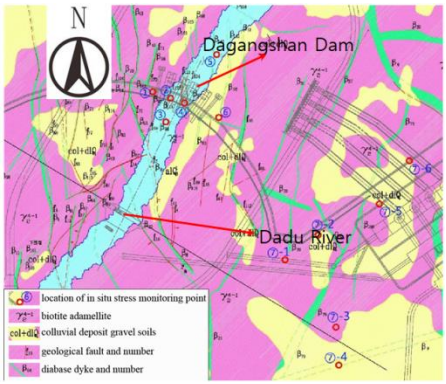

(a)

(b)

Fig. 3 A plan view of the dam layout and a top view of the slope (a) a plan view of the dam and (b) a top view of the slope

has powerful drawing functions, is employed to establish the numerical model for jointed rock mass. The cutting files in DDARF can be generated by Auto CAD and then can be operated directly. Using the optimized DDARF method, not only can users establish numerical models in bench scale, but also can work on actual engineering projects. Meanwhile, the parallel joint group and the random joint group can both be generated in the numerical model, and all types of geometric shapes on specimens, tunnels, underground caverns, mountain slopes, etc. can be established in the optimized DDARF. Fig. 1 shows an example on the numerical model establishment of an underground cavern with random joint group in Auto CAD. The failure process of fractured rock mass was analyzed during the excavation of underground cavern by means of the equivalent mechanical characteristics. DDARF method is adopted to analyze the stability of an underground cavern with random joints.

In summary, the optimized DDARF method to numerically simulate the whole failure process of jointed rock mass has the following steps:

(1) Based on the in situ geological investigations and Monte-Carlo method, the probability model for jointed rock mass can be established in terms of lognormal distribution, normal distribution, uniform distribution and negative exponential distribution;

(2) The rock joints are divided into groups according to the joint dominant occurrences. Then the corresponding geometrical parameters of rock joints (including trace length, dip angle and dip strike) can be obtained by the Monte-Carlo method;

(3) The complex numerical model with joint networks can be established through the visual interface of Auto CAD. The joint network should be continuously modified. For example, the most close-located joints can be combined together, and the joints beyond the simulated areas can be eliminated;

(4) Using the optimized DDARF method, the cutting files can be generated, which significantly reduces the tedious manual workloads and greatly improves the calculation efficiency.

The technical flowchart of optimized DDARF is shown in Fig. 2.

3. Engineering description

The Dagangshan hydropower station is located in the middle part of the Dadu River in Sichuan Province of southwestern China, as shown in Fig. 3. The Dagangshan dam is located at the middle ranch of the Dadu River flowing from north to south. The dam is a double curvature concrete dam of 210 m high, and the underground cavern of the hydropower station is located in the left bank. The dam is a double-curvature concrete with the maximum height of 210 m, and the hydropower station has a maximum output of 2,600 MW. The normal pool level is 1,130 m and the total storage capacity is $7.42 \times 10^8 m^3$.

The rock mass at the slope site mainly consists of Chengjiang period granite including medium-grained biotite monzonite granite (γ_2^{4-1}) and fine-to-medium grained syenogranite (γ_{k2}^{4-4}). *In situ* testing results reveal that the *in situ* stress values of the Dagangshan dam site are not very high, and the maximum value is 18.92 MPa.

Table 1 A statistical table of the joint fracture occurrence

(a) The characteristics of trace length				
Trace length (m)	0.4-1.0	1.0-3.0	3.0-5.0	>5.0
Percentage (%)	37	58	3	2
(b) Statistics of occurrence			(c) Statistics of spacing	
The number of groups	The dominant occurrence	Density percentage (%)	Average spacing (m)	Percentage (%)
1	194°∠3°	4-5	<0.1 m	15.1
2	177°∠81°	3-4	0.1-0.2 m	16.6
3	288°∠63°	3-4	0.2-0.4 m	35.4
4	254°∠65°	2.5-3.5	0.4-0.6 m	16.4
5	77°∠35°	2-3	0.6-0.8 m	8.4
6	Not available		>0.8	8.2

Table 2 Physico-mechanical parameters of rock masses and geological structural planes

Weathering degree of the rock mass		Fully weathered	Strongly weathered	The upper part of weakly weathered rock		The lower part of weakly weathered rock		Slightly weathered
Classification of rock mass, RQD (%)		<25		25–50	25–50	25–50	50–75	75–90
Rock mass	Cohesion *C*(MPa)	1.7		5.8		6.8		12.3
	Friction angle φ(°)	42.3		47.9		47.9		56.3
	Elastic modulus *E*(GPa)	5.7		21.7		23.9		38.8
Geological structural plane	Cohesion *C*(MPa)	0		0	0.15	0	0.15	0.2
	Friction angle φ(°)	26.6		26.6	36.8	26.6	36.8	44.4

The right bank slope is selected as the research object. The natural slope is relatively steep, which is between 45° and 60°. From the information of the previous geophysical prospecting and initial excavations, eighty-four developed faults have been found in the right bank slope, and among which F_1, f_{191}, f_{174}, f_{231} and f_{208} are determined as the relatively large faults. The number of the main developed joint sets is six. A geological map of a typical cross section in the right bank slope is shown in Fig. 4. A statistical table of the joint fracture occurrence is shown in Table 1 and the corresponding physico-mechanical parameters of rock masses and geological structural planes are shown in Table 2.

The right bank slope can be regarded as a large-scale slope with a complex geological structure, intensely unloaded and weathered rock mass, high seismic intensity as well as complicated geological and topographic conditions. Therefore, these complicated features are extremely unfavourable for jointed rock slope stability. Even at the beginning stage of excavations, big deformations, fault rupture and dislocation and excavation-induced fractures are often monitored and detected, which may result in large-scale landslide.

4. Numerical simulation on stability evaluation of the rock slope with multiple sets of random joints using the optimized DDARF

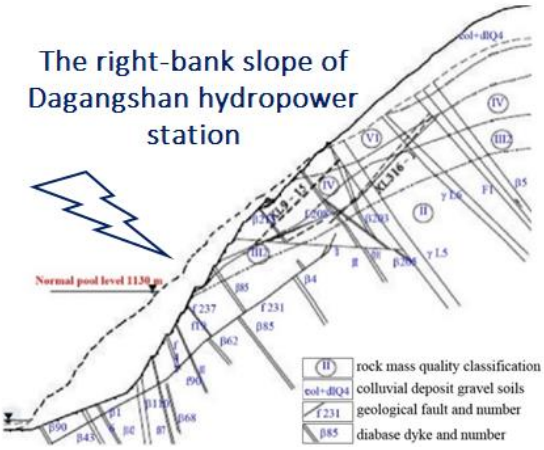

Fig. 4 A geological map of a typical cross section in the right bank slope

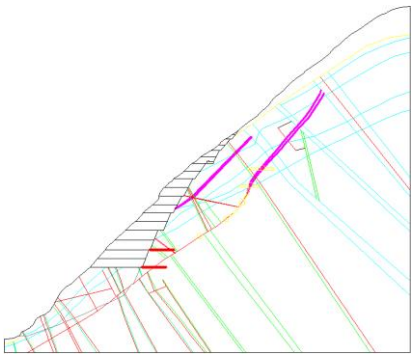

Fig. 5 A simplified geological map of the typical right bank slope in Auto CAD

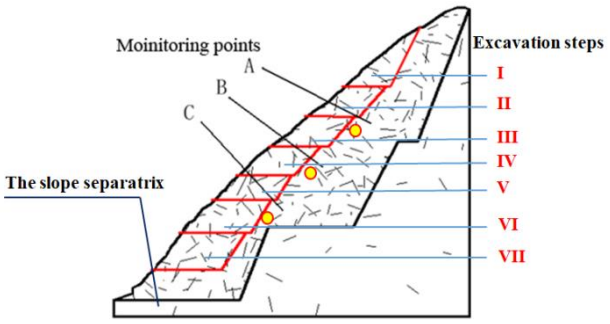

Fig. 6 Random joint network, slope separatrix, three monitoring points and seven excavation steps of the slope

4.1 Generation of multiple sets of random joints in the rock slope

After the rock mass of slope is disturbed by excavations, the mechanical properties, strength, and stability will be greatly controlled by the discontinuities in the rock mass. The geological conditions of the right bank slope in Fig. 4 are relatively complex, therefore the simplified geological features in Auto CAD are shown in Fig. 5. It can be obviously seen that most of the actual geological conditions can be found in the simplified geological figure.

According to the distribution principle of the geological structural parameters, a series of random numbers can be obtained using the Monte-Carlo method. The random numbers would be replaced with the geometric parameters

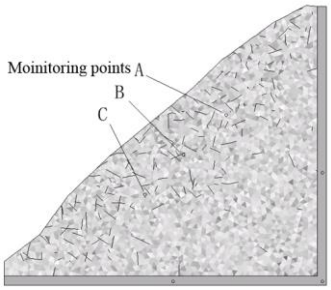

Fig. 7 The numerical model with random joint network in optimized DDARF

Table 3 Physico-mechanical parameters of the rock mass, actual joints and artificial joints in the numerical simulation

Group name	Elastic modulus (GPa)	Poisson's ratio	Cohesion (MPa)	Tensile strength (MPa)	Friction angle (°)	Dilatancy angle (°)
Rock mass	5.7	0.28	1.7	1.0	56.3	0
Actual joints	—	—	0	0	47.9	0
Artificial joints	—	—	0	0	47.9	0

of discontinuities (including trace length, dip angle and dip strike), then a series of discontinuities will be obtained and an equivalent network will be formed. As for one rock joint, it can be determined by center point coordinate (x_0, y_0), trace length (l), and the dip angle (θ). The breakpoint coordinate of the joint trace line can be expressed as below

$$\begin{cases} x = x_0 \pm \dfrac{l}{2} \times \cos\theta \\ y = y_0 \pm \dfrac{l}{2} \times \sin\theta \end{cases} \tag{4}$$

In the simulated area of the slope, the spatial distributions of the center point coordinate (x_0, y_0) obey Poission distribution. Under the two-dimensional condition, the occurrence of the structural plane is only determined by the directional angle(α), which can be obtained by the relationship between the occurrence of the structural plane and the simulated section of the jointed rock slope. Here, the trace length in the structural plane is assumed to obey normal distribution. The number of the joints is determined by the simulated area size and the number of unit areas. The final generated random joint network of the slope is shown in Fig. 6. The whole rock slope is divided into two parts by the slope separatrix shown in Fig. 6. The left part is the highly-weathered zones, thus it is filled with smaller-spacing and densely distributed random joint networks. The right part is the slightly-weathered and intact rock mass, and it is filled with some sparsely distributed random joint networks. The whole excavation works are simplified into seven excavation steps, as also shown in Fig. 6. Three monitoring points close to the excavating rock mass are selected to perform the slope stability evaluation in the numerical simulations.

4.2 Establishment of the numerical model in optimized DDARF

According to the generation of random joint network in

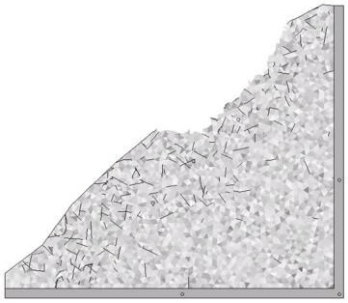

(a) Excavation step 2

(b) Excavation step 4

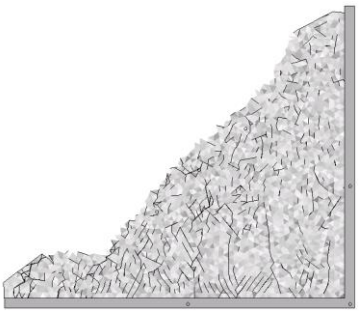

(c) Excavation step 7

Fig. 8 Numerical results of rock slope with multiple sets of random joints during excavations

the rock slope, the numerical model is established in optimized DDARF, as shown in Fig. 7. The right and bottom boundaries are confined within a perpendicular-type rigid body. The whole mountain body is 584.5 m in height and 30-45°in natural slope degree. Three monitoring points (A, B and C) are located in the upper part, middle part and lower part of the rock slope, respectively. They are selected to obtain the variations of stress, strain and displacement during excavations.

The process during generation of the random joint network is always accompanied by singular joint, which would hinder the mesh generation. After elaborate selection, these singular joints would be adjusted or eliminated. Due to the limited quantity of singular joints in the rock slope body, it will not result in great errors in the numerical simulation during excavations. Finally, the numerical model of the rock slope is divided into 6,000 triangle elements. The related physico-mechanical parameters of the rock mass, actual joints and artificial joints are listed in Table 3.

4.3 Numerical results on the rock slope with multiple sets of random joints during excavations

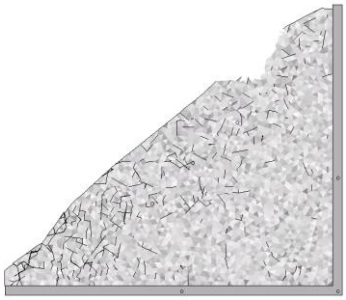

(a) Excavation step 1

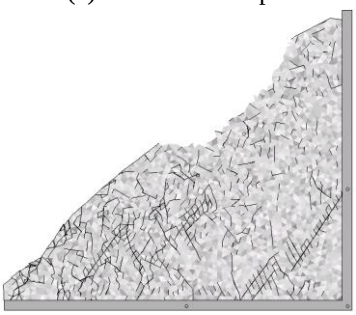

(b) Excavation step 3

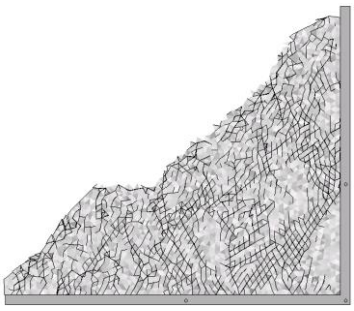

(c) Excavation step 5

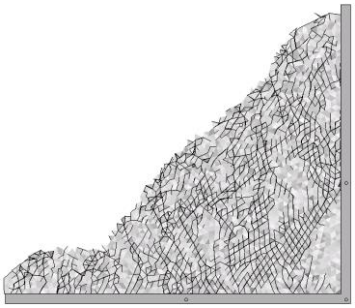

(d) Excavation step 7

Fig. 9 Numerical results of rock slope with multiple sets of random joints during excavations when the gravity coefficient is increased up to 1.4

4.3.1 Numerical results under the action of gravitational force

In this numerical simulation, the self-weight stress is only considered as the *in situ* stresses are relatively smaller. The excavations result in stress redistributions of the rock slope body. Fig. 8(a)-(c) shows the joint development in the rock slope under different excavation steps.

It can be seen that the rock slope is in a good stability state when the excavation step 2 is completed. When the excavation step 4 is finished, the inner random joints in the rock slope body begin to extend, especially in the slope foot

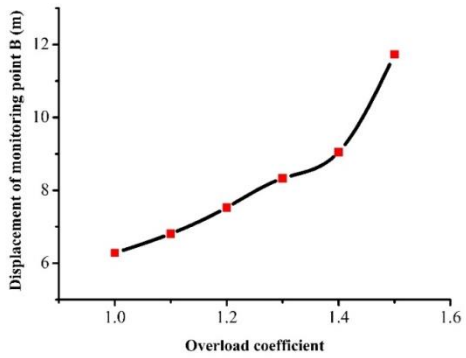

Fig. 10 The relationship between the displacement of monitoring point B and the overload coefficient in the rock slope with multiple sets of random joint network

area. And some random joints even propagate near the slope surface area. After the whole excavation steps are completed, great extensions have occurred in the inner random joints, joint propagations have also occurred among the adjacent joints, and even a small number of varying scaled cracks have been initiated in the intact rock area with sparsely distributed random joints. Overall, there are a few totally propagated joints in the rock slope body, and the rock slope is always in a stable state during the process of excavations. Under the action of gravitational force, through comparing the deformation of the perpendicular-type rigid body at the right and bottom boundary, the whole rock slope has been compressed and extended in the vertical direction and horizontal direction, respectively.

4.3.2 Numerical results under overloading tests

In order to completely perform the stability evaluation of the rock slope with multiple sets of random joint network, numerical simulations under overloading tests are also carried out. In these numerical simulations, the gravity coefficient is progressively increased by increment of 0.1. Fig. 9(a)-(d) shows the joint development in the rock slope under different excavation steps when the gravity coefficient is increased up to 1.4. When excavation step 1 is completed, the inner joints in the rock slope body initiate to extend and a preliminary scale of extension has been formed, especially in the slope foot area. When excavation step 3 is completed, the slope body has been obviously compressed in the vertical direction, and several apparent shear fractured zones have been formed. However, the remaining slope surface ready for next excavation steps and the newly formed slope surface induced by previous excavations are both in a relatively stable state. When excavation step 5 is completed, slight sliding has occurred in the blocks of slope top area. Additionally, numerous propagated joints have been generated in the remaining slope surface and the newly formed slope surface induced by previous excavations. Some blocks are also broken away from the slope body. This condition can be regarded as an instable state. When excavation step 7 is completed, the obvious sliding phenomenon has occurred in the blocks of slope top area, and the newly formed slope surface induced by all previous excavations has been almost totally occupied by propagated joint networks. The blocks sliding of the slope top area may result in large-scale sliding in the lower part of the slope surface.

As for the variation of deformation of the monitoring points, here point B is taken as an example. The relationship between the displacement of monitoring point B and the overload coefficient is shown in Fig. 10. From this curve, it can be obtained that the overload coefficient at the inflection point is 1.39. Therefore, it is concluded that the safety factor of the rock slope with multiple sets of random joint network is determined as 1.39.

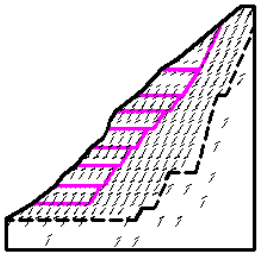

(a) The second rock slope section with two sets of regular parallel joints

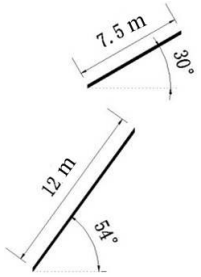

(b) Dimensions and dip angles of two sets of regular parallel joints

Fig. 11 The second rock slope section of the right bank slope with two sets of regular parallel joints

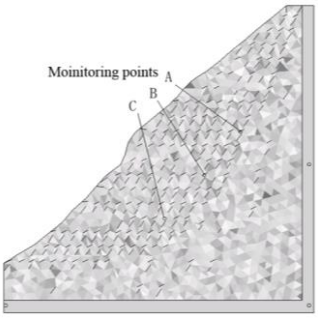

Fig. 12 Numerical model with two sets of regular parallel joint network in optimized DDARF

5. Numerical simulation on stability evaluation of the rock slope with two sets of regular parallel joints and with no joint

In order to further study the joint influences on the rock slope stability, another similar slope section in the right bank slope is also selected to perform the stability analysis. In this section, the rock joints can be simplified to be two sets of regular parallel joints. In addition, the rock stability analysis with no joint is also conducted.

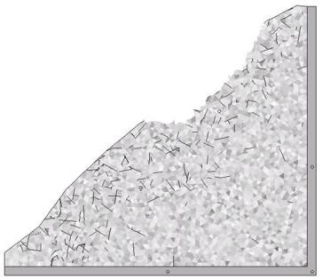

(a) Excavation step 2

(b) Excavation step 4

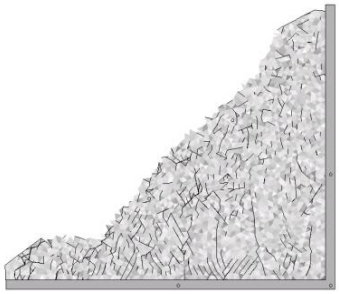

(c) Excavation step 7

Fig. 13 Numerical results of the second rock slope section with two sets of regular parallel joints during excavations

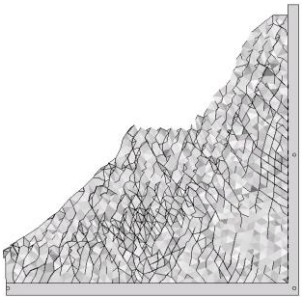

(a) Excavation step 2

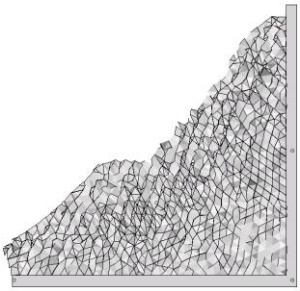

(b) Excavation step 4

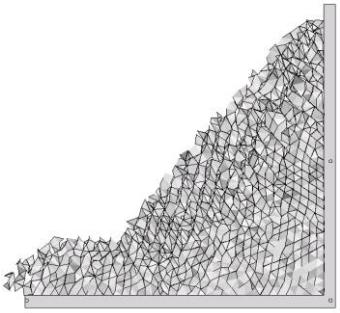

(c) Excavation step 7

Fig. 14 Numerical results of rock slope with two sets of regular parallel joints during excavations when the gravity coefficient is increased up to 2.7

5.1 Case 1: The rock slope with two sets of regular parallel joints

The second rock slope section in the right bank slope is shown in Fig. 11, which also shows the distribution of two sets of regular parallel joints. The two sets of regular parallel joints are the simplified joints based on the actual geometric parameters and distributions of joints in the rock slope. The numerical model is established and shown in Fig. 12. The whole excavation work is divided into eight steps. Three monitoring points (A, B and C) are also located in the upper part, middle part and lower part of the rock slope, respectively. They are also selected to obtain the variations of stress, strain and displacement during excavations. The related physico-mechanical parameters in the numerical simulation are provided in Table 3.

In this numerical model, the two sets of regular parallel joints have caused difficulties in generating triangular elements. Therefore, there are only 2,800 triangular elements in this numerical model. Although fewer elements may not be ideal for the model, the numerical results can still reveal the related problems on slope stability during excavations.

The first numerical simulation also only considers the self-weight of the rock slope body. Fig. 13(a)-13(c) shows the joint development in the rock slope under different excavation steps. Under the double actions of self-weight and excavation disturbance, in the beginning of excavations, the initiation of fine and long cracks occurs in the middle and lower part of the slope body, and these new cracks even propagate with the original joints. As the excavations go on, the inner joints continue to extend and propagate, and the rock slope body has been compressed in the vertical direction and extended in the horizontal direction. Several apparent shear fractured zones have been formed. When excavations are totally completed, the rock slope body is almost filled with propagated joints. A number of blocks on the slope surface have the tendency to slide down.

The second numerical simulation is the overloading test. The gravity coefficient is also progressively increased by increment of 0.1. Fig. 14(a)-(c) shows the joint development in the rock slope under different excavation steps when the gravity coefficient is increased up to 2.7. We observe that the joints in the rock slope body have been greatly propagated. In the beginning of excavations (when

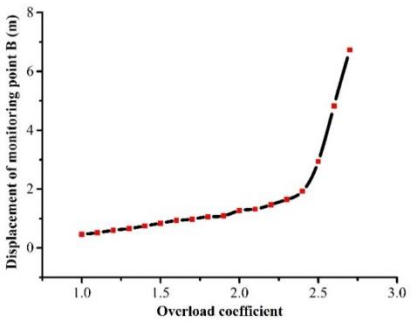

Fig. 15 The relationship between the displacement of monitoring point B and the overload coefficient in the rock slope with two sets of regular parallel joints

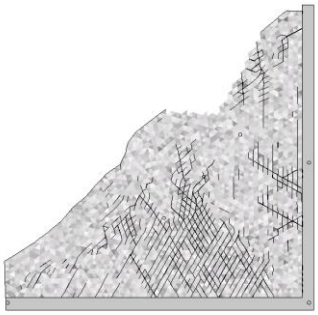

(a) Excavation step 2

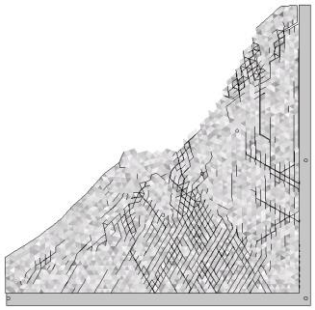

(b) Excavation step 4

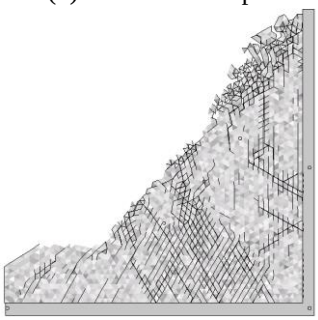

(c) Excavation step 7

Fig. 16 Numerical results of rock slope with no joint during excavations when the gravity coefficient is increased up to 5.8

excavation step 2 is completed), the blocks at the slope foot area begins to slide down. When excavation step 7 is completed, the rock slope is in a totally instable state and large-scale collapse or landside may occur at any time.

The deformation of monitoring point B is also recorded during excavations. The relationship between the displacement of monitoring point B and the overload coefficient is shown in Fig. 15. We find from the displacement history that the overload coefficient at the inflection point is 2.42. Therefore, it is concluded that the safety factor of the rock slope with two sets of regular parallel joints is determined as 2.42.

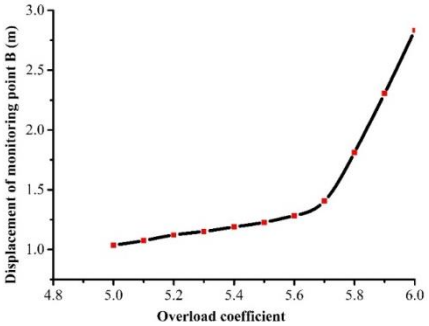

Fig. 17 The relationship between the displacement of monitoring point B and the overload coefficient in the rock slope with no joint

5.2 Case 2: The rock slope with no joint

The above two simulation schemes both consider the joint influences on the rock stability. In the next simulation, the same rock slope section with no joint will be considered. The related physico-mechanical parameters in the numerical simulation are also given in Table 3. The excavations steps are the same as that in case 1. As no joint exists in the rock slope body, the numerical model can be successfully divided into 6,000 triangular elements, which can greatly guarantee the calculation accuracy. Fig. 16(a)-(c) shows the joint development in the rock slope under different excavation steps when the gravity coefficient is increased up to 5.8. It can be concluded that the stability of the rock slope with no joint is always in a good and stable state during excavations when the overloading coefficient is gradually increased from 1.0 to 5.8. Fig. 17 exhibits the relationship between the displacement of monitoring point B and the overload coefficient. It is obtained from this figure that the overload coefficient at the inflection point is 5.68. Therefore, it is concluded that the safety factor of the rock slope with no joint is determined as 5.68.

6. Conclusions

In this paper, we present an optimized method using Discontinuous Deformation Analysis for Rock Failure (DDARF) to perform numerical investigations on the jointed rock slope stability evaluation of the Dagangshan hydropower station. The optimization in DDARF is primarily embodied in the pre-processing stage of establishing the numerical model with complex geological conditions using Auto CAD. During the numerical investigations on the stability evaluation of jointed rock slope, three calculation schemes have been taken into account in the numerical model: (I) no joint; (II) two sets of regular parallel joints; and (III) multiple sets of random joints. And the following conclusions can be drawn:

(1) The concentration areas of joint extension and propagation are primarily distributed in the newly formed slope surface induced by previous excavations under the double actions of self-weight and excavation disturbance. Results of numerical simulation can provide constructive immediate supporting schemes during excavations.

(2) During the overloading tests, greater joint extensions and propagations have occurred in the slope body in the beginning of excavations. In the final stage of excavations, the rock slope has the tendency to slide down;

(3) The numerical results from the three calculation schemes during excavations can illustrate the whole developments of crack initiation, propagation, formation of shear zones and local failures. Overloading safety factors of the three schemes are also determined as 5.68, 2.42 and 1.39, respectively. It can be concluded that the joints near the excavation surface in the rock slope body have significant influences on the slope stability during excavations. The optimized DDARF method can describe the process and details of crack initiation and propagation in a better way comparing with other numerical methods. The analysis of block deformation provides a new numerical perspective for slope simulation.

Acknowledgments

The work was supported by the National Science and Technology Support Program of China (2015BAB07B05), Shandong Provincial Natural Science Foundation, China (ZR2016EEQ01), the Fundamental Research Funds of Shandong University (2016JC007) and visiting scholar funding in 2017 of China Scholarship Council (201706225011).

References

Bishop, A.W. and Morgenstern, N. (1960), "Stability coefficients for earth slopes", *Géotechnique*, **10**, 129-150.

Bonilla-Sierra, V., Scholtès, L., Donzé, F.V. and Elmouttie, M.K. (2015), "Rock slope stability analysis using photogrammetric data and DFN-DEM modelling", *Acta Geotech.*, **10**(4), 497-511.

Cemalettin, O.A., Guzin, G.U. and Yilmaz, O. (2016), "Comparison of Hoek-Brown and Mohr-Coulomb failure criterion for deep open coal mine slope stability", *Struct. Eng. Mech.*, **60**(5), 809-828.

Chen, S.H., Xu, M.Y., Shahrour, I. and Egger, P. (2003), "Analysis of arch dams using coupled trial load and block element methods", *J. Geotech. Geoenviron.*, **129**(11), 977-986.

Chen, Y., Li, S., Zhu, W., Zhang, L. and Liu, G. (2013), "New method of ddarf network simulation and its application on highway tunnel", *J. Central South Univ.*, **44**(6), 2494-2499.

Choi, S.O. and Chung, S.K. (2004), "Stability analysis of jointed rock slopes with the barton-bandis constitutive model in UDEC", *J. Rock Mech. Min. Sci.*, **41**(3), 581-586.

Cundall, P.A. and Strack, O.D.L. (1979), "A discrete numerical model for granularassemblies", *Géotechnique*, **29**(1), 47-65.

Dai, F., Lee, C., Deng, J. and Tham, L. (2005), "The 1786 earthquake-triggered landslide dam and subsequent dam-break flood on the Dadu River, southwestern China", *Geomorphology*, **65**(3-4), 205-221.

Duncan, J.M. (1996), "State of the art: Limit equilibrium and finite element analysis of slopes", *J. Geotech. Eng.*, **122**(7), 557-596.

Florkiewicz, A. and Kubzdela, A. (2009), "Factor of safety in limit analysis of slopes", *Geomech. Eng.*, **5**(5), 283–284.

Gao, Y.F., Wu D., Zhang F., Lei, G.H., Qin, H.Y. and Qiu, Y. (2016), "Limit analysis of 3D rock slope stability with non-linear failure criterion", *Geomech. Eng.*, **10**(1), 59-76.

Guharay, A. and Baidya, D.K. (2014), "Partial safety factors for retaining walls and slopes: A reliability-based approach", *Geomech. Eng.*, **6**(2), 99-115.

Günther, A., Wienhöfer, J. and Konietzky, H. (2012), "Automated mapping of rock slope geometry, kinematics and stability with RSS-GIS", *Nat. Hazards*, **61**(1), 29-49.

Hatzor, Y.H., Arzi, A.A., Zaslavsky, Y. and Shapira, A. (2004), "Dynamic stability analysis of jointed rock slopes using DDA method: King Herod's Palace, Masada, Israel", *J. Rock Mech. Min. Sci.*, **41**(5), 813-832.

Huang, R.Q. (2009), "Some catastrophic landslides since the twentieth century in the southwest of China", *Landslides*, **6**(1), 69-81.

Huang, R.Q. and Fan, X.M. (2013), "The landslide story", *Nat. Geosci.*, **6**, 325-326.

Hungr, O., Salgado, F.M. and Byrne, P.M. (2011), "Evaluation of a three-dimensional method of slope stability analysis", *Can. Geotech. J.*, **26**(4), 679-686.

Janbu, N. (1973), *Slope Stability Computations*, Wiley, New York, U.S.A.

Ji, J. and Liao, H.J. (2014), "Sensitivity-based reliability analysis of earth slopes using finite element method", *Geomech. Eng.*, **6**(6), 545-560.

Jiang, Q.H., Qi, Z.F., Wei, W. and Zhou, C.B. (2015), "Stability assessment of a high rock slope by strength reduction finite element method", *Bull. Eng. Geol. Environ.*, **74**(4), 1153-1162.

Jiao, Y.Y., Zhang, H.Q., Tang, H.M., Zhang, X.L., Adoko, A.C. and Tian, H.N. (2014a), "Simulating the process of reservoir-impoundment-induced landslide using the extended DDA method", *Eng. Geol.*, **182**, 37-48.

Jiao, Y.Y., Zhang, H.Q., Zhang, X.L., Li, H.B. and Jiang, Q.H. (2014b), "A two-dimensional coupled hydromechanical discontinuum model for simulating rock hydraulic fracturing", *J. Numer. Anal. Met.*, **39**(5), 457-481.

Jiao, Y.Y., Zhang, X.L. and Li, T.C. (2010), *Discontinuous Deformation Analysis for Modeling Jointed Rock Failure Process*, Science Press, Beijing, China.

Latha, G.M. and Garaga, A. (2010), "Stability analysis of a rock slope in Himalayas", *Geomech. Eng.*, **2**(2), 125-140.

Li, L.C., Tang, C.A., Zhu, W.C. and Liang, Z.Z. (2009), "Numerical analysis of slope stability based on the gravity increase method", *Comput. Geotech.*, **36**(7), 1246-1258.

Li, Y., Zhou, H., Zhu, W.S., Li, S.C. and Liu, J. (2015), "Numerical investigations on slope stability using an elasto-brittle model considering fissure water pressure", *Arab. J. Geosci.*, **8**(12), 10277-10288.

Li, Y., Zhou, H., Zhu, W.S., Li, S.C. and Liu, J. (2016), "Experimental and numerical investigations on the shear behavior of a jointed rock mass", *Geosci. J.*, **20**(3), 371–379.

Liu, S.Y., Shao, L.T. and Li, H.J. (2015), "Slope stability analysis using the limit equilibrium method and two finite element methods", *Comput. Geotech.*, **63**, 291-298.

Liu, W.D. (2015), "Scientific understanding of the belt and road initiative of China and related research themes", *Prog. Geogr.*, **34**(5), 538-544.

Lu, C.Y., Tang, C.L., Chan, Y.C., Hu, J.C. and Chi, C.C. (2014), "Forecasting landslide hazard by the 3D discrete element method: A case study of the unstable slope in the Lushan hot spring district, central Taiwan", *Eng. Geol.*, **183**, 14-30.

Ministry of Water Resources of the People's Republic of China (2007), *Design Codefor Engineering Slopes in Water Resources*

and Hydropower Projects, SL386-2007, China Water Power Press, Beijing, China.
Morgenstern, N.R. and Price, V.E. (1965), "The analysis of the stability of general slip surfaces", *Geotechnique*, **15**, 79-93.
Nichol, S.L., Hungr, O. and Evans, S.G. (2011), "Large-scale brittle and ductile toppling of rock slopes", *Can. Geotech. J.*, **39**(4), 773-788.
Peng, C. (2006), *21st Century China Hydropower Engineering*, China Water Power Press, Beijing, China.
Qi, C.Q., Wu, J.M., Liu, J. and Kanungo, D.P. (2016), "Assessment of complex rock slope stability at Xiari, southwestern China", *Bull. Eng. Geol. Environ.*, **75**(2), 537-550.
Sarfarazi, V., Haeri, H. and Khaloo, A. (2016). "The effect of non-persistent joints on sliding direction of rock slopes", *Comput. Concrete*, **17**(6), 723-737.
Sarma, S.K. (1973), "Stability analysis of embankments and slopes", *Geotechnique*, **23**, 423-433.
Shi, G.H. (1988), "Discontinuous deformation analysis: A new numerical model for the statics and dynamics of block system", Ph.D. Dissertation, University of California Berkeley, Berkeley, California, U.S.A.
Shih, V. (2004), "Development, the second time around: the political logic of developing western China", *J. East Asian Stud.*, **4**(3), 427-451.
Spencer, E. (1967), "A method of analysis of the stability of embankments assuming parallel inter-slice forces", *Geotechnique*, **17**(1), 11-26.
Sun, J.P., Ning Y.J. and Z.Y. Zhao. (2011), "Comparative study of Sarma's method and the discontinuous deformation analysis for rock slope stability analysis", *Geomech. Geoeng.*, **6**(4), 1-10.
Terzi, N.U. and Selcuk, M.E. (2015), "Nonlinear dynamic behavior of pamukcay earthfill dam", *Geomech. Eng.*, **9**(1), 83-100.
Wang, C., Tannant, D.D. and Lilly, P.A. (2003), "Numerical analysis of the stability of heavily jointed rock slopes using PFC2D", *J. Rock Mech. Min. Sci.*, **40**(3), 415-424.
Wang, S.H. and Ni, P.P. (2013), "Application of block theory modeling on spatial block topological identification to rock slope stability analysis", *J. Comput. Meth.*, **11**(1), 390-400.
Xiao, L.L., Chai, B. and Yin, K.L. (2015), "Rock slope stability evaluation in a steep-walled canyon: Application to elevator construction in the Yunlong River Valley, Enshi, China", *Rock Mech. Rock Eng.*, **48**(5), 1969-1980.
Xu, W.J., Xu, Q. and Wang, Y.J. (2013), "The mechanism of high-speed motion and damming of the Tangjiashan landslide", *Eng. Geol.*, **157**, 8-20.
Yan, T.Z., Yang, S.A. and Fang, Y.L. (2000), *Landslidologies*, China University of Geosciences Press, Wuhan, China.
Yang, T.H., Shi, W.H., Wang, P.T., Liu, H.L., Yu, Q.L. and Li, Y. (2015), "Numerical simulation on slope stability analysis considering an isotropic properties of layered fractured rocks: A case study", *Arab. J. Geosci.*, **8**(8), 5413-5421.
Yang, X.L. and Pan, Q.J. (2015), "Three dimensional seismic and static stability of rock slopes", *Geomech. Eng.*, **8**(1), 97-111.
Yang, X.L. and Yin, J.H. (2004), "Slope stability analysis with nonlinear failure criterion", *J. Eng. Mech.*, **130**(3), 267-275.
Yin, Y., Wang, F. and Sun, P. (2009), "Landslide hazards triggered by the 2008Wenchuan earthquake, Sichuan, China", *Landslides*, **6**(2), 139-152.
Yu, S.J., Liu, R.Z. and Cheng, J.L. (2010), "A minimum travel time ray tracing global algorithm on a triangular net for propagating plane waves", *Appl. Geophys.*, **7**(4), 348-356.
Zaruba, Q. and Mencl, V. (1969), *Landslide and Their Control*, Elsevier, Amsterdam, Holland.
Zhang, X.L. (2007), "Study on numerical methods for modelling failure process of semi-continuous jointed rock mass", Ph.D. Dissertation, Chinese Academy of Sciences, Wuhan, China.
Zhang, X.L., Jiao, Y.Y. and Zhao, J. (2008), "Simulation of failure process of jointed rock", *J. Central South Univ. Technol.*, **15**, 888-894.
Zhao, L.H., Cao, J.Y., Zhang, Y.B. and Luo, Q. (2015), "Effect of hydraulic distribution on the stability of a plane slide rock slope under the nonlinear Barton-Bandis failure criterion", *Geomech. Eng.*, **8**(3), 391-414.
Zhao, W., Huang, R. and Yan, M. (2015). "Study on the deformation and failure modes of rock mass containing concentrated parallel joints with different spacing and number based on smooth joint model in PFC", *Arab. J. Geosci.*, **8**(10), 7887-7897.
Zheng, J., Deng, J.H., Zhang, G.Q. and Yang, X.J. (2015), "Validation of Monte Carlo simulation for discontinuity locations in space", *Comput. Geotech.*, **67**, 103-109.
Zhu, T.Z. (2009), 20th Century River Hydropower Planning in China, China Electric Power Press, Beijing, China.

CC